IEEE Access
Multidisciplinary ⋮ Rapid Review ⋮ Open Access Journal

Received November 18, 2017, accepted January 12, 2018, date of publication January 23, 2018, date of current version April 18, 2018.

*Digital Object Identifier 10.1109/ACCESS.2018.2796618*

# Throughput Analysis of Wavelet OFDM in Broadband Power Line Communications

**FREDDY A. PINTO-BENEL, (Student Member, IEEE), MANUEL BLANCO-VELASCO, (Senior Member, IEEE), AND FERNANDO CRUZ-ROLDÁN, (Senior Member, IEEE)**

Department of Teoría de la Señal y Comunicaciones, Escuela Politécnica Superior, Universidad de Alcalá, 28871 Alcalá de Henares, Spain

Corresponding author: Freddy A. Pinto-Benel (freddy.pinto@uah.es)

This work was supported by the Spanish Ministry of Economy and Competitiveness through the Project Research under Grant TEC2015-64835-C3-1-R.

**ABSTRACT** Windowed orthogonal frequency-division multiplexing (OFDM) and wavelet OFDM have been proposed as multicarrier techniques for broadband communications over the power line network by the standard IEEE 1901. The windowed OFDM has been extensively researched and employed in different fields of communication, while the wavelet OFDM has been recently recommended for the first time in a standard. This paper is aimed to show that the wavelet OFDM, which basically is an extended lapped transform-based multicarrier modulation (ELT-MCM), is a viable and attractive alternative for data transmission in hostile scenarios, such as in-home power line communications (PLC). To this end, we obtain theoretical expressions for ELT-MCM of: 1) the desired signal power; 2) the inter-symbol interference power; 3) the inter-carrier interference power; and 4) the noise power at the receiver side. These expressions are used to derive the throughput. This paper includes several computer simulations that show that ELT-MCM is an efficient alternative to improve data rates in the PLC systems.

**INDEX TERMS** Power line communications, multicarrier modulation, orthogonal frequency-division multiplexing, extended lapped transform-based multicarrier modulation, filter bank multicarrier modulation, discrete cosine transform, discrete sine transform, prototype filter.

## I. INTRODUCTION

Channel partitioning techniques have become part of several standards for broadband wireless and wireline communications. The idea behind these techniques is to convert a broadband frequency channel into a set of overlapping and (nearly) orthogonal frequency-flat subchannels [1] aimed at sharing the media among users. Orthogonal Frequency Division Multiplexing (OFDM), with or without windowing, is the most widely recommended technique and employs cyclic prefix (CP) or zeros as redundant samples to carry out the channel partition [2]. Recently, filter bank multicarrier (FBMC) has attracted a great deal of research attention, with the difference that the partitioning is performed by means of pulse shaping, with good properties in time and frequency, with no additional redundant samples [3]. FBMC is now proposed as an attractive alternative to OFDM as the modulation technique of the fifth generation of wireless networks (5G) [4]–[9].

The popularity of power line communications (PLC) for smart grids, for in-vehicle applications, and for outdoors and in-home data communication systems, has grown a great deal [10]–[19]. It can be a good solution for the 'last mile' problem, since it provides broadband communication to isolated places where other communication systems are not in place, and for the 'last inch' problem, since it implements indoor high-speed networks [20]. IEEE Std 1901 [21] defines a standard for broadband over power line (BPL) devices via electric power lines. All classes of BPL devices are considered for the use of this standard, including BPL devices used for smart energy or in-vehicle applications.

The physical layer (PHY) procedures included in IEEE 1901 specify either a windowed OFDM or a wavelet OFDM as multicarrier modulation (MCM) schemes. Although the latter scheme is referred to as wavelet OFDM, the recommended system is not based on wavelet, it is a class of FBMC based on the Extended Lapped Transform (ELT) [16], [22]. For this reason, hereinafter we will refer to wavelet OFDM also as ELT-MCM.

It is well known that one important drawback of OFDM is its insertion of redundancy, which reduces the throughput.

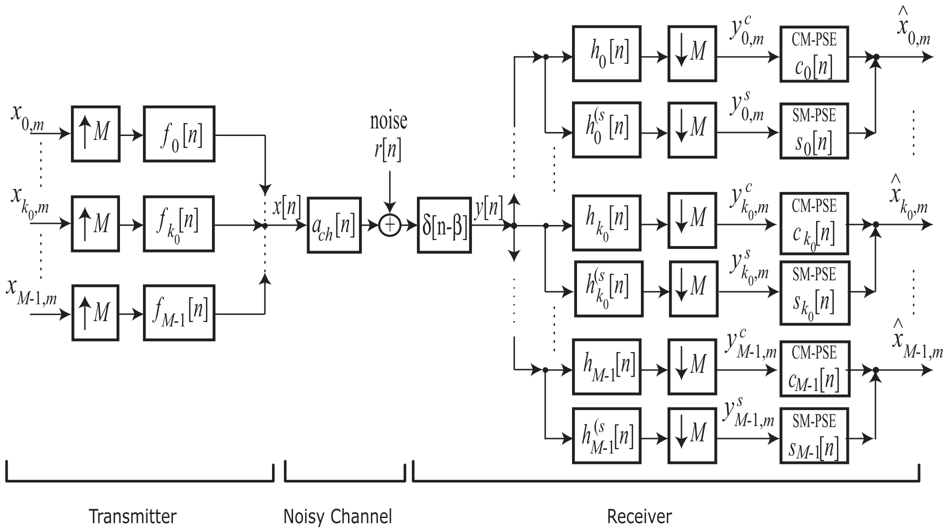


**FIGURE 1.** General block diagram of an ELT-MCM with ASCET.

As an alternative, FBMC is a viable and attractive solution for communications over the mains network, because it does not require any kind of redundancy, it has higher robustness in noisy environments, greater spectral separation, and reduced adjacent subchannel interference, among others. However, channel equalization represents one of the most challenging issues and plays an important role in the PLC receivers based on FBMC, chiefly since the PLC channel varies in both frequency and time, and experiences deep notches [23].

Since OFDM with and without windowing has been recommended in other standards, e.g., HomePlug AV [24], it has received widespread attention by researchers. In this respect, there have been previous studies of the capacity and throughput of OFDM-based systems. For instance, in [25] the discrete multi-tone (DMT) capacity was analyzed. The performance of windowed OFDM systems was studied in [26] and [27]. Recent literature has proposed contributions with specific emphasis on OFDM/OQAM (FBMC/OQAM) [25], [26], [28], [29]. A special case of FBMC, based on the conventional modulation [30], has been studied in [31]–[33]. To the best of the authors' knowledge, the study of the throughput for the system based on the ELT and deployed by IEEE 1901, is still an open problem. The main purpose of this paper is to derive theoretical expressions for the wavelet OFDM system (or ELT-MCM), also including an Adaptive Sine-modulated/Cosine-modulated filter bank Equalizer for Transmultiplexer (ASCET) [16], [34]. Finally, a comparison of the throughputs for windowed OFDM and ELT-MCM is included, considering an in-home PLC scenario.

The rest of this paper is organized as follows. In Section II, the ELT-MCM system is briefly presented. In Section III theoretical expressions for the power of the desired signal, of the inter-symbol interference (ISI), of the inter-carrier interference (ICI), and of the noise, all at the receiver side, are derived. In Section IV, we study the throughput. Section V contains some simulation results. Section VI provides our conclusions.

## II. FILTER BANK MULTICARRIER TRANSCEIVER

Fig. 1 shows the block diagram of the filter bank multicarrier transceiver detailed in [16] and considered in the present paper. The baseband ELT-MCM physical layer recommended in [21] is the following transmitting filter (for the $k$th subband, for $0 \leq k \leq M-1$):

$$f_k[n] = \sqrt{\frac{2}{M}} \cdot p[n] \cdot \cos\left[\left(k+\frac{1}{2}\right)\frac{\pi}{M}\left(n+\frac{M+1}{2}\right)\right] \times \cos(\theta_k), \quad (1)$$

where $0 \leq n \leq N$, $M$ is the number of subbands, $p[n]$ is the prototype filter with length equal to $N+1 = 2\kappa M$, $\kappa$ is the overlapping factor, and $\theta_k$ is a phase constant equal to 0 or $\pi$. Expression (1), excluding the term $\cos(\theta_k)$, is nothing but the ELT synthesis filters introduced by Malvar [22]. For the above transmitting bank, the reception system can be implemented as the time reflection of the transmission bank [16]:

$$h_k[n] = \sqrt{\frac{2}{M}} \cdot p[n] \cdot \cos\left[\left(k+\frac{1}{2}\right)\frac{\pi}{M} \times \left(N-n+\frac{M+1}{2}\right)\right] \cdot \cos(\theta_k). \quad (2)$$

With regard to $p[n]$, different prototype filters are proposed in the standard [21] for the cases of $M = 512$, 1024 and 2048 subchannels, and for an overlapping factor $\kappa$ equal to 2 or 3. It is worth noting that the proposed prototype filters have even symmetry ($p[N-n] = p[n]$). The standard does not provide expressions that allow designers to quickly obtain the corresponding coefficients, but in [16] it is shown that these prototype filters belong to a family of windows proposed by Malvar [22] which has the perfect reconstruction (PR) property in the context of filter banks.

In order to compensate for the channel effects, the ASCET system can be used [35]. Its use for ELT-MCM was proposed in [16], and the impulse responses of the receiving filters of the sine modulated filter bank (SMFB) are given by

$$h_k^s[n] = \sqrt{\frac{2}{M}} \cdot p[n] \cdot \sin\left[\left(k+\frac{1}{2}\right)\frac{\pi}{M} \times \left(N-n+\frac{M+1}{2}\right)\right] \cdot \cos(\theta_k). \quad (3)$$

For more details of the transceiver configuration and for a quick and efficient way of implementing the whole system of Fig. 1 by means of polyphase filters, we refer the reader to [16].

## III. ANALYTICAL EXPRESSIONS

In Fig. 1, let us consider the discrete-time transmitted signal given by

$$x[n] = \sum_{k\in\mathbb{K}_{on}} \sum_{m\in\mathbb{Z}} x_{k,m} \cdot f_k[n-mM], \quad (4)$$

where $\mathbb{K}_{on} \subseteq \{0, \cdots, M-1\}$ is the set of active subchannels defined by the tone mask [21], and $x_{k,m}$ are the symbols in the subcarrier-time position $(k, m)$, assumed to be zero-mean wide-sense stationary (WSS) processes. In particular, the variance $\sigma_x^2$ is assumed to be identical for all $x_{k,m}$, which are independent and identically distributed for every $k$ in $\mathbb{K}_{on}$. We assume that the PLC channel can be modeled as a time-invariant frequency selective channel:

$$a_{ch}[n] = \sum_{l=0}^{L-1} a_l \cdot \delta[n-l], \quad (5)$$

where $L$ is the length of the channel. We also assume that there is no significant variation during a frame transmission. The received signal is given by

$$y[n] = \sum_{l=0}^{L-1} a_l \cdot x[n-l-\beta] + r[n-\beta], \quad (6)$$

where $r[n]$ is additive noise and $\beta$ is a delay included to obtain proper system operation. In this paper, we assume the noise to be additive white Gaussian noise with zero mean and variance $\sigma_r^2$. Lastly, the signal at the $k_0$-subcarrier output can be written as

$$y_{k_0,n}^c = \sum_{\tau=0}^{N} h_{k_0}[\tau] \cdot y[nM-\tau] = \sum_{\tau=0}^{N} h_{k_0}[\tau] \times \sum_{l=0}^{L-1} a_l \cdot \sum_{k\in\mathbb{K}_{on}} \sum_{m\in\mathbb{Z}} x_{k,m} \cdot f_k[nM-\tau-l-\beta-mM] + \sum_{\tau=0}^{N} h_{k_0}[t] \cdot r[nM-\beta-\tau]. \quad (7)$$

In the following subsections, we will obtain the signal-to-interference-plus-noise ratio (SINR) under the reasonable assumption that the number of subcarriers used is quite large, so that the interference on a given subcarrier is normally distributed [27].

### A. TRANSMITTING OVER A CHANNEL WITHOUT NOISE

Noise apart, the output symbol at the position $(k_0, m_0)$ can be written as

$$y_{k_0,m_0}^c = \sum_{k\in\mathbb{K}_{on}} \sum_{m\in\mathbb{Z}} x_{k,m} \sum_{l=0}^{L-1} a_l \cdot G_{k_0,m_0}^c(k, m, l), \quad (8)$$

where

$$G_{k_0,m_0}^c(k, m, l) = \sum_{\tau=0}^{N} f_k[m_0 M - \tau - l - \beta - mM] \cdot h_{k_0}[\tau].$$

The expression (8) can be separated into the signal, $(k, m) = (k_0, m_0)$, and interference, $(k, m) \neq (k_0, m_0)$. The first part gives rise to the signal of interest

$$\Psi_{k_0,m_0}^c = x_{k_0,m_0} \sum_{l=0}^{L-1} a_l \cdot G_{k_0,m_0}^c(k_0, m_0, l) = x_{k_0,m_0} \cdot Q_{k_0,m_0}^c(k_0, m_0), \quad (9)$$

and the second one to the inter-symbol interference (ISI)

$$I_{k_0,m_0}^c = \sum_{\substack{m\in\mathbb{Z}\\ m\neq m_0}} x_{k_0,m} \sum_{l=0}^{L-1} a_l \cdot G_{k_0,m_0}^c(k_0, m, l) = \sum_{\substack{m\in\mathbb{Z}\\ m\neq m_0}} x_{k_0,m} \cdot Q_{k_0,m_0}^c(k_0, m), \quad (10)$$

and the inter-carrier interference (ICI)

$$J_{k_0,m_0}^c = \sum_{\substack{k\in\mathbb{K}_{on}\\ k\neq k_0}} \sum_{m\in\mathbb{Z}} x_{k,m} \cdot \sum_{l=0}^{L-1} a_l \cdot G_{k_0,m_0}^c(k, m, l) = \sum_{\substack{\mathbb{K}_{on}\\ k\neq k_0}} \sum_{m\in\mathbb{Z}} x_{k,m} \cdot Q_{k_0,m_0}^c(k, m), \quad (11)$$

where

$$Q_{k_0,m_0}^c(k, m) = \sum_{l=0}^{L-1} a_l \cdot G_{k_0,m_0}^c(k, m, l).$$

Therefore, the cosine modulated filter bank (CMFB) output symbol can be expressed as

$$y_{k_0,m_0}^c = \Psi_{k_0,m}^c + I_{k_0,m_0}^c + J_{k_0,m_0}^c. \quad (12)$$

Following the same reasoning, the SMFB output symbol at the position $(k_0, m_0)$ is

$$y_{k_0,m_0}^s = \Psi_{k_0,m}^s + I_{k_0,m_0}^s + J_{k_0,m_0}^s, \quad (13)$$

where the expressions of the signal of interest, ISI and ICI are similar to (9)-(11), but $G_{k_0,m_0}^c(k, m, l)$ is replaced by

$$G_{k_0,m_0}^s(k, m, l) = \sum_{\tau=0}^{N} f_k[m_0 M - \tau - l - \beta - mM] \cdot h_{k_0}^s[\tau],$$

and

$$Q^s_{k_0,m_0}(k_0,m_0) = \sum_{l=0}^{L-1} a_l \cdot G^s_{k_0,m_0}(k_0,m_0,l).$$

### B. NOISE EFFECTS

Taking the noise[1] into consideration, (12) and (13) can be rewritten as

$$y^c_{k_0,m_0} = \Psi^c_{k_0,m_0} + I^c_{k_0,m_0} + J^c_{k_0,m_0} + r^c_{k_0,m_0}, \quad (14)$$
$$y^s_{k_0,m_0} = \Psi^s_{k_0,m_0} + I^s_{k_0,m_0} + J^s_{k_0,m_0} + r^s_{k_0,m_0}, \quad (15)$$

where

$$r^c_{k_0,m_0} = \sum_{\tau=0}^{N} h_{k_0}[\tau] \cdot r[m_0M - \beta - \tau], \quad (16)$$
$$r^s_{k_0,m_0} = \sum_{\tau=0}^{N} h^s_{k_0}[\tau] \cdot r[m_0M - \beta - \tau]. \quad (17)$$

### C. THE SINR OF THE 0-ASCET

In the 0-ASCET [34], [35], the cosine-modulated per-subcarrier equalizer (CM-PSE) and the sine-modulated (SM) PSE are constants[2]:

$$c_k[n] = c_k, \quad s_k[n] = s_k.$$

Thus, the demodulated $(k_0, m_0)$th symbol in the absence of noise can be written as

$$\begin{aligned}\hat{x}_{k_0,m_0} &= y^c_{k_0,m_0} \cdot c_{k_0} + y^s_{k_0,m_0} \cdot s_{k_0} \\ &= \underbrace{\Psi^c_{k_0,m_0} \cdot c_{k_0} + \psi^s_{k_0,m_0} \cdot s_{k_0}}_{\Psi^T_{k_0,m_0}} \\ &\quad + \underbrace{I^c_{k_0,m_0} \cdot c_{k_0} + I^s_{k_0,m_0} \cdot s_{k_0}}_{I^T_{k_0,m_0}} \\ &\quad + \underbrace{J^c_{k_0,m_0} \cdot c_{k_0} + J^s_{k_0,m_0} \cdot s_{k_0},}_{J^T_{k_0,m_0}} \end{aligned} \quad (18)$$

where $\Psi^T_{k_0,m_0}$, $I^T_{k_0,m_0}$ and $J^T_{k_0,m_0}$ are the signal and the total interference parts at the $(k_0, m_0)$th symbol. The signal power can then be calculated as the second central moment:

$$\begin{aligned}P_\Psi(k_0) &= E\left[\left|\Psi^T_{k_0,m_0}\right|^2\right] \\ &= \sigma_x^2 \left|Q^c_{k_0,m_0}(k_0,m_0) \cdot c_{k_0} + Q^s_{k_0,m_0}(k_0,m_0) \cdot s_{k_0}\right|^2. \end{aligned} \quad (19)$$

where $E[\cdot]$ is the expected value. Next, the intersymbol interference power is obtained as

$$\begin{aligned}P_{\mathrm{ISI}}(k_0) &= E\left[\left|I^T_{k_0,m_0}\right|^2\right] \\ &= \sigma_x^2 \sum_{\substack{m\in\mathbb{Z} \\ m\neq m_0}} \Big|Q^c_{k_0,m_0}(k_0,m) \cdot c_{k_0} \\ &\qquad + Q^s_{k_0,m_0}(k_0,m) \cdot s_{k_0}\Big|^2. \end{aligned} \quad (20)$$

On the other hand, the total intercarrier interference power can be obtained as

$$\begin{aligned}P_{\mathrm{ICI}}(k_0) &= E\left[\left|J^T_{k_0,m_0}\right|^2\right] \\ &= \sigma_x^2 \sum_{\substack{\mathbb{K}_{on} \\ k\neq k_0}} \sum_{m\in\mathbb{Z}_0} \Big|Q^c_{k_0,m_0}(k,m) \cdot c_{k_0} \\ &\qquad + Q^s_{k_0,m_0}(k,m) \cdot s_{k_0}\Big|^2. \end{aligned} \quad (21)$$

The noise at the demodulated $(k_0, m_0)$th symbol can be expressed as

$$\begin{aligned}P_r(k_0) &= E\left[\left|r^c_{k_0,m_0} \cdot c_{k_0} + r^s_{k_0,m_0} \cdot s_{k_0}\right|^2\right] \\ &= \sigma_r^2 \sum_{\tau=0}^{N} \left|c_{k_0} \cdot h_{k_0}[\tau] + s_{k_0} \cdot h^s_{k_0}[\tau]\right|^2. \end{aligned} \quad (22)$$

Considering (19), (20), (21), and (22), the SINR at the $k_0$th subcarrier is obtained as

$$\mathrm{SINR}(k_0) = \frac{P_\Psi(k_0)}{P_{\mathrm{ISI}}(k_0) + P_{\mathrm{ICI}}(k_0) + P_r(k_0)}. \quad (23)$$

The theoretical expressions to obtain the SINR for a higher order ASCET are derived in Appendix.

## IV. THROUGHPUT ANALYSIS

In this section, we obtain the maximal data rate of Wavelet OFDM. Previously, we show the expressions derived in [26] for windowed OFDM.

### A. WINDOWED OFDM PHY

The theoretical throughput can be calculated by the following expression:

$$R = \Delta_f \sum_{k\in\mathbb{K}'_{on}} \frac{M}{M+GI} \cdot C(k), \quad (24)$$

where $\Delta_f$ is the subcarrier spacing, $\mathbb{K}'_{on}$ is the set of active subcarriers, $GI$ is the length of the guard interval in samples, and $C(k)$ is the maximal data rate for the $k$th subchannel, which can be calculated by means of the following expression:

$$C(k) = \log_2\left(1 + \frac{\mathrm{SINR}(k)}{\Gamma}\right). \quad (25)$$

$\Gamma$ is the SINR gap that, when $2^{2K}$-QAM constellation is used, is defined by

$$\Gamma \approx \frac{1}{3}\left[Q^{-1}\left(\frac{\mathrm{SER}}{4}\right)^2\right], \quad (26)$$

[1] The channel noise in an in-home PLC channel results from the contribution of different noises (impulsive or background) and narrowband interferences [36], [37].

[2] Background material on the design of an ASCET for ELT-MCM can be found in [16].

where SER stands for the symbol error rate and $Q^{-1}(\cdot)$ is the inverse tail probability of the standard normal distribution [1], [3]. For $\Gamma = 1$, $C(k)$ is the capacity of the $k$th subchannel.

Assuming single tap subcarrier equalization and that both the noise and the input signals are independent and Gaussian distributed, the SINR of the windowed OFDM system is [26]:

$$\mathrm{SINR}(k_0) = \frac{\sigma_x^2(k_0)|H_{k_0}|^2}{\sigma_n^2(k_0) + P_{ICI+ISI}^{Wofdm}(k_0)}, \tag{27}$$

where $\sigma_x^2(k_0)$ denotes the variance of the transmitted symbols; $\sigma_n^2(k_0)$, $H_{k_0}$, and $P_{ICI+ISI}^{Wofdm}(k_0)$ are the PLC noise level, the frequency channel coefficient, and the interference power, respectively, all the above on the $k$th subcarrier.

### B. WAVELET OFDM PHY

As in the previous case, the ELT-MCM throughput can be obtained using (24). Since this technique does not need a guard interval, and provided we assume that the interference power on a given subcarrier is normally distributed, the throughput formula yields

$$R = \Delta_f \sum_{k \in \mathbb{K}_{on}} \log_2\left(1 + \frac{\mathrm{SINR}(k)}{\Gamma}\right), \tag{28}$$

where the SINR is given by (23) or (38), and $\Gamma$ is also the SINR gap. Since IEEE 1901 [21] proposes the PAM as the primary mapping for the ELT-MCM PHY, and assuming that an $M$-QAM is like 2 $M$-PAM independent modulations [1], [3], we have

$$\Gamma \approx \frac{1}{3}\left[Q^{-1}\left(\frac{\mathrm{SER}}{2}\right)\right]^2. \tag{29}$$

## V. SIMULATION RESULTS

The theoretical throughput of the ELT-MCM and windowed OFDM system will be compared in this section considering an in-home PLC scenario. There are several approaches for modeling in-home PLC channels [10], [36], [38]–[40]. In this paper, we focus our attention on the model proposed in [38], which is a statistical approach that synthesizes different classes with a finite number of multi-path components. Our simulations consisted in averaging the outcomes of 100 transmissions through different impulse response realizations representative of class 1 (strong signal attenuation), class 5 (medium signal attenuation) and class 9 (little signal attenuation), which have been computed using the script available on-line in [41]. In addition, we assume that the channel remains constant during each multicarrier symbol, and perfect channel knowledge is also assumed at the receiver. Furthermore, there is no kind of error-correcting-code. In particular, we assume the following conditions for each multicarrier scheme:

- Wavelet OFDM PHY: Following the specifications deployed by IEEE 1901, the ELT-MCM system employs the prototype filter recommended for $M = 512$ subcarriers and $\kappa = 2$. There are 360 active subcarriers (used for data modulation) in the range from 1.8 MHz to 28 MHz, and the frequency spacing ($\Delta_f$) is 61.03515625 kHz.
- FFT OFDM PHY: The specifications of the windowed OFDM system are also based on [21]. This system uses 4096 subcarriers with up to 1974 usable subcarriers in the range of [1.8 − 50] MHz, and the subcarrier spacing is approximately 24.414 kHz. Support for carriers above 30 MHz is optional. Of the subcarriers below 30 MHz, 917 are active. In addition, the standard fixes a mandatory payload symbol guard interval (GI) equal to 556, 756 or 4712 samples. In order to ensure a fair comparison, approximately equal occupied bandwidth should be considered for both transceivers. For this reason, we assume in our simulations $M = 4096$ and 917 active subcarriers for the windowed OFDM. Furthermore, the GI is chosen to be 756 to provide good system performance and to not penalize this transceiver.

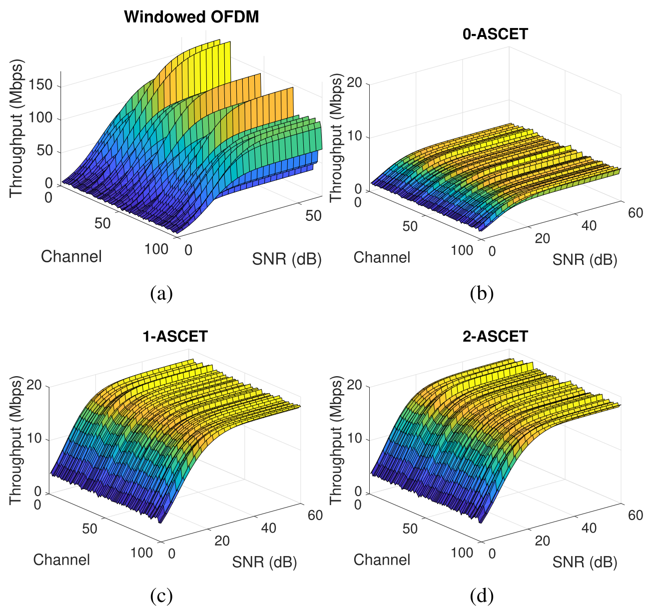


**FIGURE 2.** Comparison of (a) FFT OFDM PHY (windowed OFDM) with (b) 0-ASCET, (c) 1-ASCET and (d) 2-ASCET Wavelet OFDM PHY (ELT-MCM) in the presence of Class 9 channels.

Following the same process as in [25] and [26], ELT-MCM will be evaluated with 0-ASCET (1-tap), 1-ASCET (3-tap), and 2-ASCET (5-tap), while a zero-forcing equalizer will be used in windowed OFDM.

In the first simulation, the windowed OFDM throughput is compared with that of the wavelet OFDM, over class 9 in-home PLC channels (little signal attenuation). Fig. 2 depicts the theoretical throughput obtained under these conditions. As can be appreciated, a significant difference can be seen: Windowed OFDM outperforms ELT-MCM, almost tripling the throughput at high SNR values. Moreover, since the PLC channel is one of the most hostile channels, the 0-ASCET is not enough to compensate for the channel distortion.

In the second comparison, we investigate the performance of both multicarrier schemes under the same conditions as

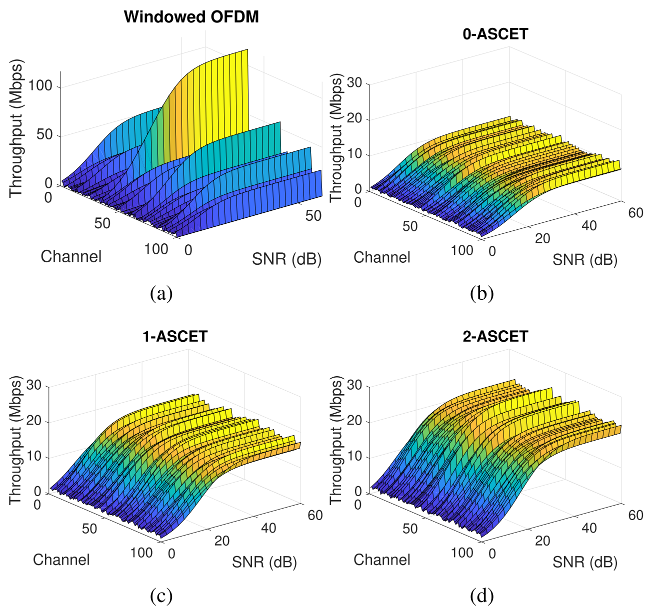


**FIGURE 3.** Comparison of (a) FFT OFDM PHY with (b) 0-ASCET, (c) 1-ASCET and (d) 2-ASCET Wavelet OFDM PHY in the presence of Class 5 channels.

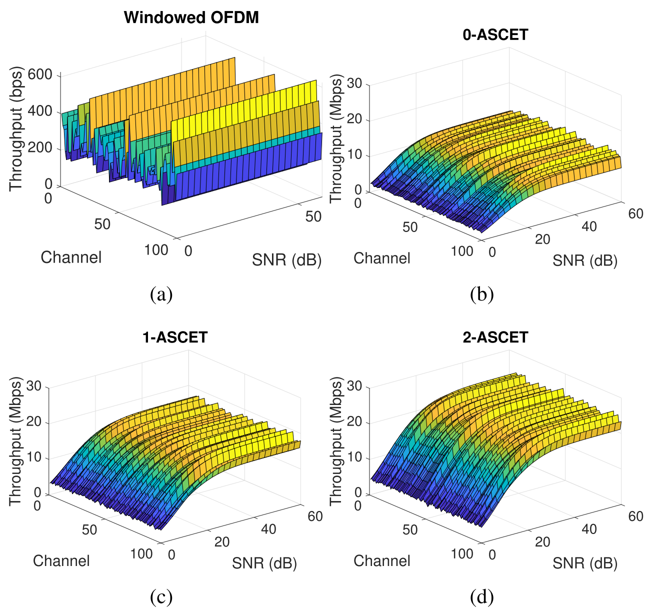


**FIGURE 4.** Comparison of (a) FFT OFDM PHY with (b) 0-ASCET, (c) 1-ASCET and (d) 2-ASCET Wavelet OFDM PHY in the presence of Class 1 channels.

the first experiment, but in the presence of PLC channels of class 5 (medium signal attenuation). Fig. 3 shows the resulting throughputs, and as can be seen, the highest values are achieved by the ELT-MCM system with 2-ASCET. These results are obtained when 1-ASCET or 2-ASCET are employed. Actually, the ELT-MCM throughput associated with 2-ASCET is 179.5% higher for SNR=20 dB.

As third scenario, both multicarrier schemes have been analyzed in the same conditions than in the first simulations but with class 1 PLC channels (strong signal attenuation).

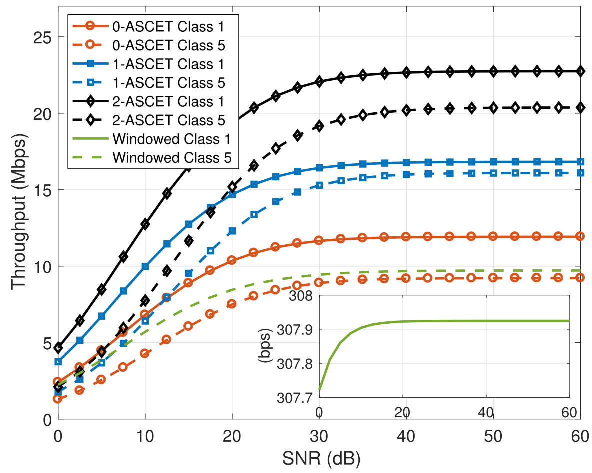


**FIGURE 5.** Mean value of throughput in presence of Class 1 and Class 5 channels, assuming AWGN as channel noise.

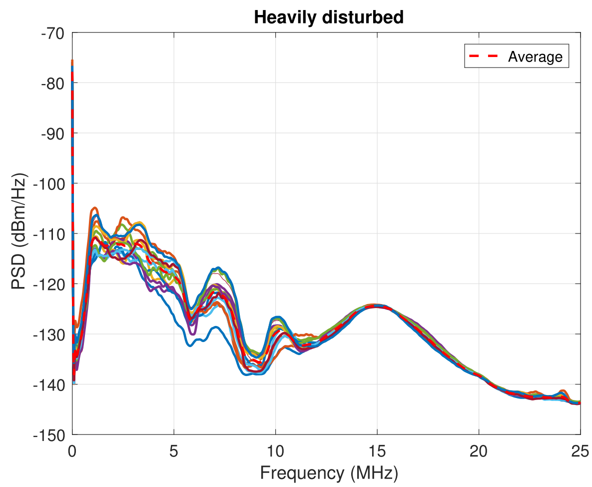


**FIGURE 6.** Background noise PSD related to a heavily disturbed in-home channel.

As shown in Fig. 4, the throughput of windowed OFDM system is considerably reduced and it is outperformed by the ELT-MCM, which shows better results than those shown in the first simulation. Finally, to easily prove the gain related to ELT-MCM over windowed OFDM, the mean value of the data rate related to the second and third simulations is shown in Fig. 5.

In the following set of experiments, the AWGN has been replaced by PLC background noise (BGN). BGN is the noise associated with a heavily disturbed channel, and it has been modeled as strong BGN following [37]. Its power spectral density is depicted in Fig. 6.

In this example, the resulting throughput is obtained once again over class 9 in-home PLC channels for both windowed OFDM and ELT-MCM. Fig. 7 depicts the theoretical throughput obtained under these conditions: windowed OFDM outperforms ELT-MCM in the same way as it did with AWGN, tripling the throughput.

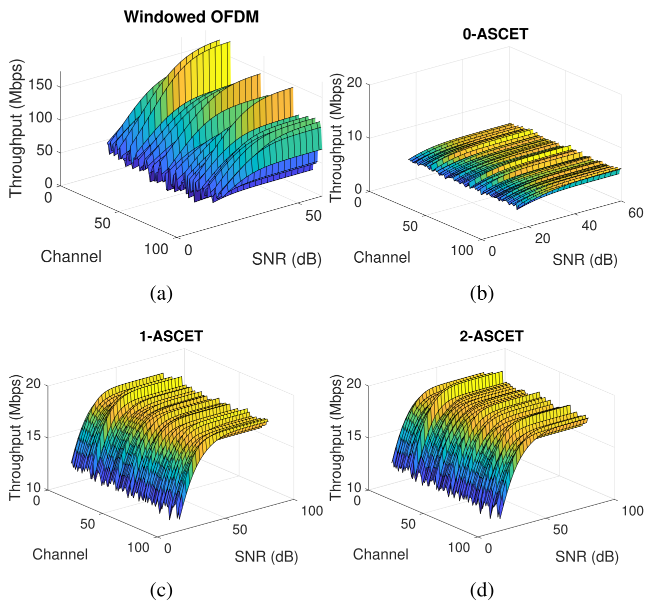


**FIGURE 7.** Comparison of (a) FFT OFDM PHY with (b) 0-ASCET, (c) 1-ASCET and (d) 2-ASCET Wavelet OFDM PHY in the presence of Class 9 channels and strong BGN.

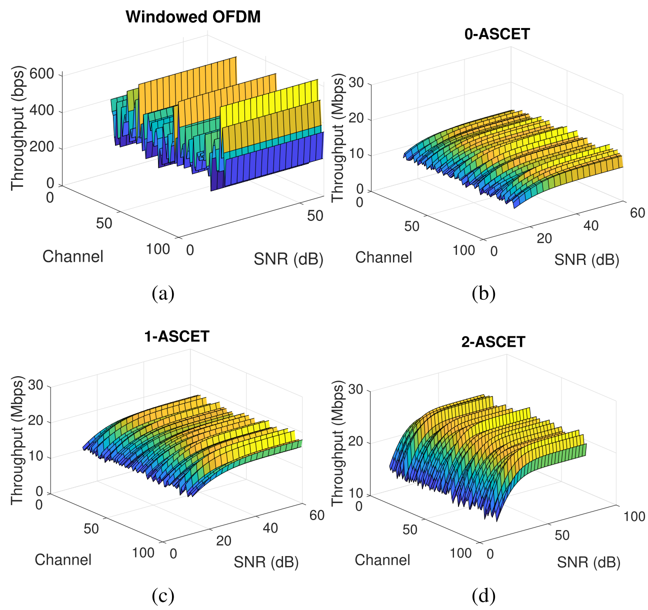


**FIGURE 9.** Comparison of (a) FFT OFDM PHY with (b) 0-ASCET, (c) 1-ASCET and (d) 2-ASCET Wavelet OFDM PHY in the presence of Class 1 channels and strong BGN.

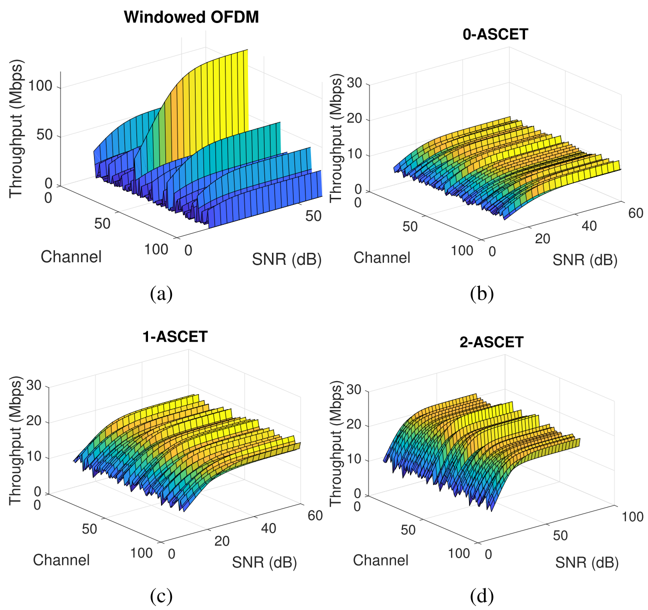


**FIGURE 8.** Comparison of (a) FFT OFDM PHY with (b) 0-ASCET, (c) 1-ASCET and (d) 2-ASCET Wavelet OFDM PHY in the presence of Class 5 channels and strong BGN.

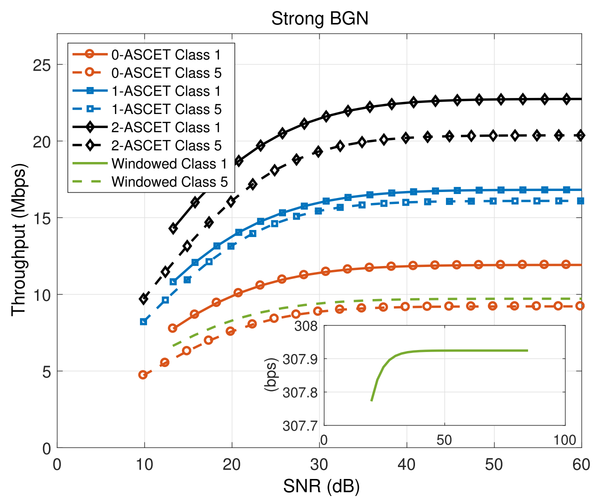


**FIGURE 10.** Mean value of throughput in presence of Class 1 and Class 5 channels, assuming BGN as channel noise.

We investigate now the performance of both multicarrier schemes over PLC channels of class 5 under strong BGN. The resulting throughputs are shown in Fig. 8, and as can be seen, the highest values are achieved by the ELT-MCM system with 2-ASCET. Actually, the ELT-MCM throughput associated with 2-ASCET is 156% higher for SNR=20 dB.

Finally, both multicarrier schemes have been compared over class 1 PLC channels. As shown in Fig. 9, the throughput of windowed OFDM system is considerably reduced and it is outperformed by the ELT-MCM. To easily prove the gain associated to the ELT-MCM system in the above set of simulations, the mean value of the throughput in the presence of Class 5 and Class 1 channels is depicted in Fig. 10.

Based on the experiments, it can be appreciated that the ELT-MCM performs better than windowed OFDM when the signal attenuation increases (more hostile channels). This phenomenon can be explained analyzing the interference power ($P_{ISI} + P_{ICI}$) of both multicarrier schemes. Fig. 11 represents the interference power of windowed OFDM and ELT-MCM assuming a maximum allowed power spectral density of $-55$ dBm/Hz (defined by the standard) and the first channel realization. It can be seen how the windowed

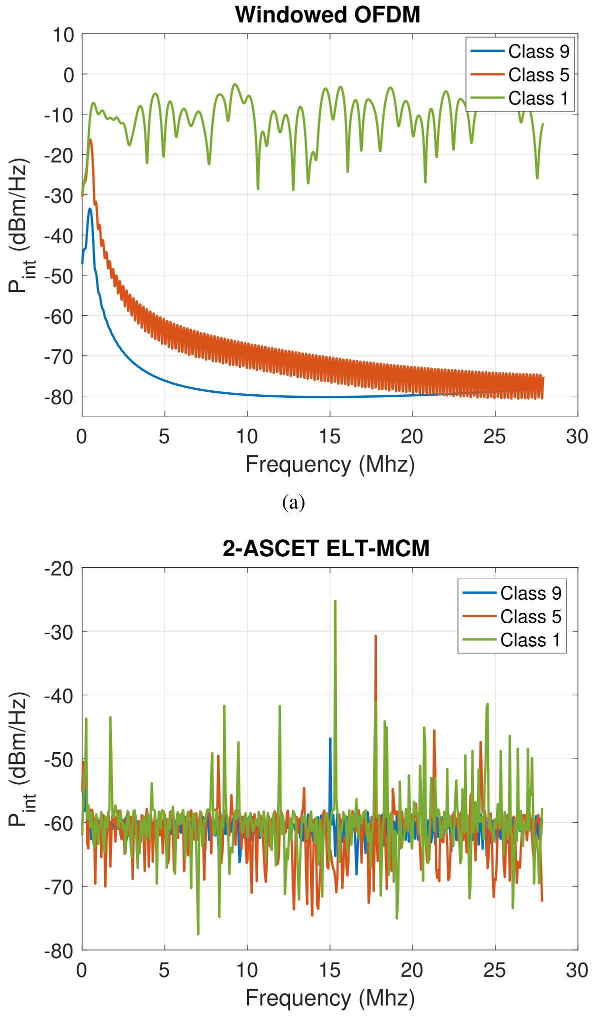


**FIGURE 11. (a) FFT OFDM PHY and (b) ELT-MCM interference power in each PLC channel.**

OFDM interference power rises when the channel hostility rises too, reaching an average of $-10$ dBm/Hz for the PLC channel class 1 (66 dB higher than the interference power obtained for the class 9). On the other hand, the ELT-MCM interference power remains more uniform for little, middle and strong signal attenuation, proving that wavelet OFDM is more robust to hostile channel than windowed OFDM. Furthermore, the throughput of windowed OFDM varies considerably among the channel tested, e.g., from 64 Mbps to 125 Kbps as shown in Fig. 3(a). Meanwhile, the performance of ELT-MCM is more homogeneous, achieving throughput between 19 Mbps and 11 Mbps under the same conditions (see Fig. 3(d)).

## VI. CONCLUSION

Wavelet OFDM is one of the multicarrier techniques deployed by the IEEE P1901 working group for broadband PLC. This paper has derived theoretical expressions for the different powers, corresponding to the desired signal, as well as to the intersymbol and the intercarrier interferences, and the noise, which are present at the receiver side for this kind of FBMC. With these expressions, the throughput of wavelet OFDM for baseband communications has been calculated. A performance comparison with windowed OFDM has also been provided, on the basis of simulations. In terms of throughput, wavelet OFDM is a viable and attractive solution because it has outperformed the windowed OFDM in hostile PLC channels, even though using fewer active subcarriers.

## APPENDIX

### THE SINR OF THE $L_A$-ASCET

The simplest equalizer with only one coefficient per subcarrier does not provide good performance in hostile channels. In order to improve its performance, the multiplications employed in 0-ASCET must be replaced by FIR filters, i.e.,

$$c_k[n] = \sum_{\mu=-L_A}^{L_A} c_{k,\mu} \cdot \delta[n-\mu],$$

$$s_k[n] = \sum_{\mu=-L_A}^{L_A} s_{k,\mu} \cdot \delta[n-\mu],$$

leading to a new equalizer of higher order, referred to as the $L_A$-order ASCET, and denoted by $L_A$-ASCET [16], [34], [35].

In this case, the demodulated $(k_0, m_0)$th symbol, in the absence of noise when the system uses a $L_A$-ASCET, is

$$\hat{x}_{k_0,m_0} = \sum_{\mu=-L_A}^{L_A} \sum_{k\in\mathbb{K}_{on}} \sum_{m\in\mathbb{Z}} x_{k,m} \cdot \Big( Q^c_{k_0,m_0-\mu}(k,m) \cdot c_{k_0,\mu} + Q^s_{k_0,m_0-\mu}(k,m) \cdot s_{k_0,\mu} \Big). \tag{30}$$

As in the previous case, the equations can be split into two groups: the signal $(k,m) = (k_0,m_0)$ and the interferences $(k,m) \neq (k_0,m_0)$. For the first group,

$$\Psi^T_{k_0,m_0} = \sum_{\mu=-L_A}^{L_A} x_{k_0,m_0} \cdot \Big( Q^c_{k_0,m_0-\mu}(k_0,m_0) \cdot c_{k_0,\mu} + Q^s_{k_0,m_0-\mu}(k_0,m_0) \cdot s_{k_0,\mu} \Big), \tag{31}$$

includes the desired symbol. Otherwise, the interference part can be defined as

$$I^T_{k_0,m_0} = \sum_{\mu=-L_A}^{L_A} \sum_{\substack{m\in\mathbb{Z}\\ m\neq m_0}} x_{k_0,m} \cdot \Big( Q^c_{k_0,m_0-\mu}(k_0,m) \cdot c_{k_0,\mu} + Q^s_{k_0,m_0-\mu}(k_0,m) \cdot s_{k_0,\mu} \Big), \tag{32}$$

and

$$J_{k_0,m_0} = \sum_{\mu=-L_A}^{L_A} \sum_{\substack{k\in\mathbb{K}_{on}\\ k\neq k_0}} \sum_{m\in\mathbb{Z}} x_{k,m} \times \Big( Q^c_{k_0,m_0-\mu}(k,m) \cdot c_{k_0,\mu} + Q^s_{k_0,m_0-\mu}(k,m) \cdot s_{k_0,\mu} \Big). \tag{33}$$

The desired signal power can be expressed as

$$P_\Psi(k_0) = \sigma_x^2 \sum_{\mu=-L_A}^{L_A} \left| Q^c_{k_0,m_0-\mu}(k_0, m_0) \cdot c_{k_0,\mu} + Q^s_{k_0,m_0-\mu}(k_0, m_0) \cdot s_{k_0,\mu} \right|^2. \tag{34}$$

On the other hand, the interference power can be obtained as

$$P_{\mathrm{ISI}}(k_0) = \sigma_x^2 \sum_{\mu=-L_A}^{L_A} \sum_{\substack{m\in\mathbb{Z}\\ m\neq m_0}} \left| Q^c_{k_0,m_0-\mu}(k_0, m) \cdot c_{k_0,\mu} + Q^s_{k_0,m_0-\mu}(k_0, m) \cdot s_{k_0,\mu} \right|^2, \tag{35}$$

and

$$P_{\mathrm{ICI}}(k_0) = \sigma_x^2 \sum_{\mu=-L_A}^{L_A} \sum_{\substack{k\in\mathbb{K}_{on}\\ k\neq k_0}} \sum_{m\in\mathbb{Z}} \left| Q^c_{k_0,m_0-\mu}(k, m) \cdot c_{k_0,\mu} + Q^s_{k_0,m_0-\mu}(k, m) \cdot s_{k_0,\mu} \right|^2. \tag{36}$$

The noise power can be calculated as

$$P_r(k_0) = \sigma_r^2 \sum_{\tau=0}^{N+2L_A} \left| h_{k_0,\mu}[\tau] + h^s_{k_0,\mu}[\tau] \right|^2, \tag{37}$$

where

$$h_{k_0,\mu}[n] = h_{k_0}[n] * c_k[n],$$
$$h^s_{k_0,\mu}[n] = h^s_{k_0}[n] * s_k[n].$$

As a result, (34), (35), (36) and (37) allow obtaining the SINR at the $k_0$th subcarrier:

$$\mathrm{SINR}(k_0) = \frac{P_\Psi(k_0)}{P_{\mathrm{ISI}}(k_0) + P_{\mathrm{ICI}}(k_0) + P_r(k_0)}. \tag{38}$$

## ACKNOWLEDGMENT

The authors would like to thank the anonymous Reviewers and the Associate Editors for their constructive suggestions which have helped in improving the paper.

## REFERENCES

[1] J. M. Cioffi, *Chapter 4: Multi-Channel Modulation*. Stanford, CA, USA: Stanford Univ., Jan. 2018. [Online]. Available: https://web.stanford.edu/group/cioffi/doc/book/chap4.pdf
[2] Y. G. Li and G. L. Stuber, Eds., *Orthogonal Frequency Division Multiplexing for Wireless Communications*. New York, NY, USA: Springer, 2006.
[3] Y.-P. Lin, S.-M. Phoong, and P. P. Vaidyanathan, *Filter Bank Transceivers for OFDM and DMT Systems*. Cambridge, U.K.: Cambridge Univ. Press, 2010.
[4] B. Farhang-Boroujeny, "Filter bank multicarrier modulation: A waveform candidate for 5G and beyond," *Adv. Elect. Eng.*, Dec. 2014, Art. no. 482805.
[5] H. Bogucka, P. Kryszkiewicz, and A. Kliks, "Dynamic spectrum aggregation for future 5G communications," *IEEE Commun. Mag.*, vol. 53, no. 5, pp. 35–43, May 2015.
[6] S. M. J. A. Tabatabaee and H. Zamiri-Jafarian, "Per-subchannel joint equalizer and receiver filter design in OFDM/OQAM systems," *IEEE Trans. Signal Process.*, vol. 64, no. 19, pp. 5094–5105, Oct. 2016.
[7] D. Gregoratti and X. Mestre, "Uplink FBMC/OQAM-based multiple access channel: Distortion analysis under strong frequency selectivity," *IEEE Trans. Signal Process.*, vol. 64, no. 16, pp. 4260–4272, Aug. 2016.
[8] E. Kofidis, "Preamble-based estimation of highly frequency selective channels in FBMC/OQAM systems," *IEEE Trans. Signal Process.*, vol. 65, no. 7, pp. 1855–1868, Apr. 2017.
[9] H. Lin, "Flexible configured OFDM for 5G air interface," *IEEE Access*, vol. 3, pp. 1861–1870, 2015.
[10] L. Lampe, A. M. Tonello, and T. G. Swart, Eds., *Power Line Communications: Principles, Standards and Applications from Multimedia to Smart Grid*, 2nd ed. Hoboken, NJ, USA: Wiley, 2016.
[11] K. M. Rabie and E. Alsusae, "On improving communication robustness in PLC systems for more reliable smart grid applications," *IEEE Trans. Smart Grid*, vol. 6, no. 6, pp. 2746–2756, Nov. 2015.
[12] F. H. Juwono, Q. Guo, Y. Chen, L. Xu, D. D. Huang, and K. P. Wong, "Linear combining of nonlinear preprocessors for OFDM-based power-line communications," *IEEE Trans. Smart Grid*, vol. 7, no. 1, pp. 253–260, Jan. 2016.
[13] T. Zheng, M. Raugi, and M. Tucci, "Time-invariant characteristics of naval power-line channels," *IEEE Trans. Power Del.*, vol. 27, no. 2, pp. 858–865, Apr. 2012.
[14] R. Ma, H.-H. Chen, Y.-R. Huang, and W. Meng, "Smart grid communication: Its challenges and opportunities," *IEEE Trans. Smart Grid*, vol. 4, no. 1, pp. 36–46, Mar. 2013.
[15] M. P. Tcheou *et al.*, "The compression of electric signal waveforms for smart grids: State of the art and future trends," *IEEE Trans. Smart Grid*, vol. 5, no. 1, pp. 291–302, Jan. 2014.
[16] F. Cruz-Roldán, F. A. Pinto-Benel, J. D. O. del Campo, and M. Blanco-Velasco, "A wavelet OFDM receiver for baseband power line communications," *J. Franklin Inst.*, vol. 353, no. 7, pp. 1654–1671, May 2016.
[17] P. Poudereux, A. Hernández, R. Mateos, F. A. Pinto-Benel, and F. Cruz-Roldán, "Design of a filter bank multi-carrier system for broadband power line communications," *Signal Process.*, vol. 128, pp. 57–67, Nov. 2016.
[18] C. Cano, A. Pittolo, D. Malone, L. Lampe, A. M. Tonello, and A. G. Dabak, "State of the art in power line communications: From the applications to the medium," *IEEE J. Sel. Areas Commun.*, vol. 34, no. 7, pp. 1935–1952, Jul. 2016.
[19] L. Zhang, H. Ma, D. Shi, P. Wang, G. Cai, and X. Liu, "Reliability oriented modeling and analysis of vehicular power line communication for vehicle to grid (V2G) information exchange system," *IEEE Access*, vol. 5, pp. 12449–12457, 2017.
[20] A. Majumder and J. Caffery, Jr., "Power line communications: An overview," *IEEE Potentials Mag.*, vol. 23, no. 4, pp. 4–8, Oct./Nov. 2004.
[21] *IEEE Standard for Broadband Over Power Line Networks: Medium Access Control and Physical Layer Specifications*, IEEE Standard 1901-2010, Dec. 2010, pp. 1–1586.
[22] H. S. Malvar, *Signal Processing With Lapped Transforms*. Norwood, MA, USA: Artech House, 1992.
[23] M. Mohammadi *et al.*, "Measurement study and transmission for in-vehicle power line communication," in *Proc. IEEE ISPLC*, Dresden, Germany, 2009, pp. 73–78.
[24] *HomePlug AV White Paper*. [Online]. Available: https://www.solwise.co.uk/downloads/files/hpav-white-paper_050818.pdf
[25] H. Lin and P. Siohan, "Capacity analysis for indoor PLC using different multi-carrier modulation schemes," *IEEE Trans. Power Del.*, vol. 25, no. 1, pp. 113–124, Jan. 2010.
[26] P. Achaichia, M. Le Bot, and P. Siohan, "OFDM/OQAM: A solution to efficiently increase the capacity of future PLC networks," *IEEE Trans. Power Del.*, vol. 26, no. 4, pp. 2443–2455, Oct. 2011.
[27] T. N. Vo, K. Amis, T. Chonavel, and P. Siohan, "Achievable throughput optimization in OFDM systems in the presence of interference and its application to power line networks," *IEEE Trans. Commun.*, vol. 62, no. 5, pp. 1704–1715, May 2014.
[28] A. Rezazadeh-Reyhani and B. Farhang-Boroujeny, "Capacity analysis of FBMC-OQAM systems," *IEEE Commun. Lett.*, vol. 21, no. 5, pp. 999–1002, May 2017.
[29] H. Wang, X. Wang, L. Xu, and W. Du, "Hybrid PAPR reduction scheme for FBMC/OQAM systems based on multi data block PTS and TR methods," *IEEE Access*, vol. 4, pp. 4761–4768, 2016.
[30] P. P. Vaidyanathanm, *Multirate Systems and Filter Banks*. Englewood Cliffs, NJ, USA: Prentice-Hall, 1993.

[31] L. Lin and B. Farhang-Boroujeny, "Cosine-modulated multitone for very-high-speed digital subscriber lines," *EURASIP J. Appl. Signal Process.*, p. 019329, Dec. 2006.

[32] D. Umehara, H. Nishiyori, and Y. Morihiro, "Performance evaluation of CMFB transmultiplexer for broadband power line communications under narrowband interference," in *Proc. IEEE Int. Symp. Power Line Commun. Appl. (ISPLC)*, Mar. 2006, pp. 50–55.

[33] K. Izumi, D. Umehara, and S. Denno, "Performance evaluation of wavelet OFDM using ASCET," in *Proc. IEEE Int. Symp. Power Line Commun. Appl. (ISPLC)*, Mar. 2007, pp. 246–251.

[34] J. Alhava and M. Renfors, "Adaptive sine-modulated/cosine-modulated filter bank equalizer for transmultiplexers," in *Proc. Eur. Conf. Circuit Theory Design*, Espoo, Finland, 2001, pp. 337–340.

[35] A. Viholainen, J. Alhava, and M. Renfors, "Efficient implementation of complex modulated filter banks using cosine and sine modulated filter banks," *EURASIP J. Appl. Signal Process.*, Dec. 2006, Art. no. 058564.

[36] M. Zimmermann and K. Dostert, "Analysis and modeling of impulsive noise in broad-band powerline communications," *IEEE Trans. Electromagn. Compat.*, vol. 44, no. 1, pp. 249–258, Feb. 2002.

[37] J. A. Cortés, L. Díez, F. Cañete, and J. Sánchez-Martínez, "Analysis of the indoor broadband power-line noise scenario," *IEEE Trans. Electromagn. Compat.*, vol. 52, no. 4, pp. 849–858, Nov. 2010.

[38] A. M. Tonello, S. D'Alessandro, and L. Lampe, "Cyclic prefix design and allocation in bit-loaded OFDM over power line communication channels," *IEEE Trans. Commun.*, vol. 58, no. 11, pp. 3265–3276, Nov. 2010.

[39] M. Antoniali, A. M. Tonello, M. Lenardon, and A. Qualizza, "Measurements and analysis of PLC channels in a cruise ship," in *Proc. IEEE Int. Symp. Power Line Commun. Appl. (ISPLC)*, Udine, Italy, Apr. 2011, pp. 102–107.

[40] F. J. Cañete, J. A. Cortés, L. Díez, and J. T. Entrambasaguas, "A channel model proposal for indoor power line communications," *IEEE Commun. Mag.*, vol. 49, no. 12, pp. 166–174, Dec. 2011.

[41] A. Tonello. (2010). *Brief Tutorial on the Statistical Top-Down PLC Channel Generator*. [Online]. Available: http://www.diegm.uniud.it/tonello/plcresearch.html


**FREDDY A. PINTO-BENEL** (S'15) was born in Arequipa, Perú, in 1990. He received the B.S. degree in telecommunications engineering and the M.Sc. degree in information technology and communications from the University of Alcalá, Spain, in 2013 and 2014, where he is currently pursuing the Ph.D. degree in information technology and communications with the Department of Signal Theory and Communications. His current research interests include digital signal processing, medium access techniques, and multirate systems applied to broadband digital communications.

**MANUEL BLANCO-VELASCO** (S'00–M'05–SM'10) received the Engineering degree from the Universidad de Alcalá, Madrid, Spain, in 1990, the M.Sc. degree in communications engineering from the Universidad Politécnica de Madrid, Spain, in 1999, and the Ph.D. degree from the Universidad de Alcalá in 2004. From 1992 to 2002, he was with the Circuits and Systems Department, Universidad Politécnica de Madrid, as an Assistant Professor. In 2002, he joined the Signal Theory and Communications Department, Universidad de Alcalá, where he is currently an Associate Professor. His main research interests are biomedical signal processing and communications.

**FERNANDO CRUZ-ROLDÁN** (M'98–SM'06) received the degree in technical telecommunication engineering from the Universidad de Alcalá (UAH), Spain, in 1990, the degree in telecommunication engineering from the Universidad Politécnica de Madrid (UPM), Spain, in 1996, and the Ph. D. degree in electrical engineering from UAH in 2000. He received the Universidad de Alcalá Prize for the most outstanding doctoral dissertation in the engineering discipline.

He joined the Department of Ingeniería de Circuitos y Sistemas, UPM, in 1990, where he was an Assistant Professor from 1993 to 2003. From 1998 to 2003, he was a Visiting Lecturer with UAH. In 2003, he joined UAH as an Associate Professor, where he has been a Professor with the Signal Theory and Communications Department since 2009.

His teaching and research interests are in digital signal processing, filter design, and multirate systems applied to subband coding and digital communications.